Hydrol. Earth Syst. Sci. Discuss., 9, 5085–5119, 2012
www.hydrol-earth-syst-sci-discuss.net/9/5085/2012/
doi:10.5194/hessd-9-5085-2012

Hydrology and
Earth System
Sciences
Discussions

Hydrogeological characterisation of a glacially affected barrier island – the North Frisian Island of Föhr

T. Burschil[1], **W. Scheer**[2], **R. Kirsch**[2], **and H. Wiederhold**[1]

[1]Leibniz Institute for Applied Geophysics LIAG, Hannover, Germany
[2]State Agency for Agriculture, Environment and Rural Areas of the Federal State Schleswig-Holstein LLUR, Geological Survey, Flintbek, Germany

Received: 11 April 2012 – Accepted: 13 April 2012 – Published: 19 April 2012

Correspondence to: T. Burschil (thomas.burschil@liag-hannover.de)

Published by Copernicus Publications on behalf of the European Geosciences Union.

Abstract

We present the application of geophysical investigations to characterise and improve the geological/hydrogeological model through the estimation of petrophysical parameters for groundwater modelling. Seismic reflection and airborne electromagnetic surveys in combination with borehole information enhance the 3-D geological model and allow a petrophysical interpretation of the subsurface.

The North Sea Island of Föhr has a very complex underground structure what was already known from boreholes. The local waterworks use a freshwater body embedded in saline groundwater. Several glaciations disordered the Youngest Tertiary and Quaternary sediments by glaciotectonic thrust-faulting as well as incision and refill of glacial valleys. Both underground structures have a strong impact on the distribution of freshwater bearing aquifers. An initial hydrogeological model of Föhr was built from borehole data alone and was restricted to the southern part of the island where in the sandy areas of the Geest a large freshwater body was formed. We improved the geological/hydrogeological model by adding data from different geophysical methods, e.g. airborne electromagnetics (EM) for mapping the resistivity of the entire island, seismic reflections for detailed cross sections in the groundwater catchment area, and geophysical borehole logging for calibration of these measurements. An integrated evaluation of the results from the different geophysical methods yields reliable data.

To determinate petrophysical parameter about 18 borehole logs, more than 75 m deep, and nearby airborne EM inversion models were analyzed concerning resistivity. We establish an empirical relation between measured resistivity and hydraulic conductivity for the specific area – the North Sea island of Föhr. Five boreholes concerning seismic interval velocities discriminate sand and till.

The interpretation of these data was the basis for building the geological/hydrogeological 3-D model. We fitted the relevant model layers to all geophysical and geological data and created a consistent 3-D model. This model is the fundament

for groundwater simulations considering forecasted changes in precipitation and sea level rise due to climate change.

1 Introduction

Increasing awareness of the secondary effects of climate change brings the groundwater situation of the North Sea coast region in the focus of research, especially under the aspect of ensuring the water supply of the future. The rising interest in impacts of climate change on groundwater demands a better understanding of groundwater systems (Green et al., 2011; Holman et al., 2012). Especially saltwater intrusion into groundwater systems is considered to be a primary climate change impact on water status (European Commission, 2009). On the barrier islands of the German North Sea coast the groundwater situation is characterized by the saltwater environment. Additionally, glacial overprinting of the sedimentary layers leads to a complex geological/hydrogeological situation, e.g. on the North Frisian Island of Föhr. Unlike the East Frisian Islands (e.g. Sulzbacher et al., 2012) the North Frisian Islands are not typical barrier islands but inclose a Geest core (Sect. 2).

In preparation of groundwater modelling regarding effects of climate change for the North Frisian Island of Föhr, a 3-D geological model was established. To enable a better understanding of the geological and hydrogeological situation and to identify important hydraulic structures potentially affecting the groundwater flow system, an intensive geophysical investigation plan was carried out. The survey included 306 km of airborne electromagnetic profiles (SkyTEM) and 10 km of seismic reflection lines. The connection of the surface methods to the existing boreholes of the waterworks was assured by vertical seismic profiling and existing well logs. The combination of these tools turned out to be extremely efficient for geological and geophysical mapping and characterization of the subsurface including the distribution of freshwater and saltwater.

In this paper we describe how the understanding of the local geological and hydrogeological situation is significantly improved by the geophysical surveys. Especially the resistivity data from electromagnetic induction measurements offer important large-scale constraints for the geological model. To avoid misinterpretations of the resistivity a careful analysis of resistivity and petrography from borehole logs was carried out. For the area of the Geest, where the recharge of fresh groundwater takes place, all available boreholes deeper than 75 m have been taken into account. Due to the good database, a correlation of geophysical and petrophysical parameter was possible leading to an empirical relationship of electrical and hydraulical properties valid for this specific site. Priority in interpretation is in rock/soil properties and not in the chemical status of the pore fluid.

2 Geological and hydrogeological background

For a better understanding of the hydrogeological situation the sedimentation history is shortly summarized (Gripp, 1964; Gürs, 2005; StUA Schleswig, 2006). Föhr is the second largest German island in the North Sea, located in the North Frisian part of the Wadden Sea (Fig. 1a). The landscape of the area was mainly formed during the glacial epoch (Saalian and Weichselian glaciations) and the post glacial time (Holocene) of the Quaternary age. The genesis of the Pre-Quaternary strata was influenced by the sedimentation in the Northern German Basin (e.g. Littke et al., 2008). Föhr, as a part of this area of subsidence, is placed on top of a succession of about 4 km heavy layers of sedimentary rocks that have been deposited during the past 280 million years. Since Cretaceous age there had been constant marine conditions for sedimentation in the area that did not change until the Youngest Tertiary. For this reason, marine clay is found as the dominating deposits in Tertiary up to Miocene. In Pliocene a regression of the sea leads over to a change from marine to terrestrial facies. The sedimentation changed from clayey to sandy deposits, caused by increasing transport of coarse grained material into the region by a widely braided river system that had its origin in the Baltic-Scandinavian area (Gürs, 2005). At the end of Pliocene age sandy material (Kaolin Sand) covered the whole landscape when a change in the global climate marked the beginning of the Pleistocene in the Quaternary age. During the glacial stages the processes of erosion and sedimentation have been caused by the action of glaciers and meltwaters. In Northern Germany especially the glaciers of different glacial stages have deeply eroded the underlying strata and formed an expansive system of tunnel valleys that were refilled with glacial deposits and are buried today. Additionally the Pre-Quaternary underground was tectonically disturbed by glacial pressure and thrust in many areas (Aber and Ber, 2007).

The ice front of the last glaciation, the Weichselian stage, did not reach the region at the North Sea coast so that in the beginning of the Holocene the landscape was covered by Saalian moraine areas and outwash plains. Weichselian sediments are restricted to only some minor occurrences of meltwater sand. In the end of the Pleistocene the sea level of the North Sea was about 100 m below the present-day height. During the marine transgression in Holocene the coastline was moving eastward while the old landscape was more and more flooded by the sea. The eroded material was transported and deposed by tidal currents. Tidal mud deposits, settled during high tide, were accumulated and formed large marsh land areas, which are protected by dikes since about 1000 yr. Several heavy floods in historical time caused the lost of large parts of the former mainland area and the breakup into the tidal flat areas of the North Frisian Wadden Sea with the islands as we can see them today.

The landscape of Föhr can be divided into two parts. The south of the island is mainly built up by sand and till of Saalian age which are the remains of the ancient Saalian land-surface. This area, the Geest, has elevations up to 12 m a.s.l. (above sea level) (Fig. 1b). The northern part consists of flat marsh land where Holocene tidal mud deposits cover the Pleistocene sediments (Fig. 1c).

The Quaternary and the Pliocene and Miocene strata of the Younger Tertiary were object of the current investigations. The geological cross section (Fig. 2) shows the layer succession of the underground of the island down to −120 m m.s.l. (mean sea level). In the southern part of the cross section a buried valley was encountered where the Quaternary deposits cut deeply into the older sediments. The Pliocene sand and the Miocene clay have been strongly tectonically influenced by glacial thrust.

Due to the high groundwater recharge in the sandy areas of the Geest in the southern part of the island, a large freshwater body was formed. Investigations have shown that freshwater can be found down to more than −80 m m.s.l. in the central parts of the Geest. There are two waterworks which supply the demand for drinking water on Föhr. The production wells mostly have their filters in the surface near Pleistocene aquifers. In addition, there are two deep wells of the waterworks in the eastern part of the island extracting groundwater from the Pliocene aquifer (Kaolin sand).

In the flat marsh areas in northern part of the island only a thin layer of freshwater overlays the saltwater.

3 Materials and methods

For the preparation of a geological/hydrogeological model a better understanding of the upper 300 m of the underground is needed. The methods used were chosen according to their convenience for structural and parametrical information for the hydrogeological model. A 3-D overview can be done by airborne electromagnetic survey, 2-D seismic surveys generate a more detailed structural image of the underground and boreholes as well as borehole measurements contribute in-situ 1-D information (Fig. 1d). A combined analysis supports and stabilizes the data interpretation of each method and is the basis for a reliable interpretation.

3.1 Airborne electromagnetic data

Electromagnetic induction (EM) is the most valuable tool for hydrogeological studies, because the measurements of electrical conductivity respond to both lithologic and water-chemistry variations (Paine and Minty, 2005). Through EM induction eddy currents are created, therefore no contact with the ground is required. Thus airborne application is possible. Airborne electromagnetic (AEM) systems allow a fast mapping of the resistivity distribution of the underground (Fountain, 1998; Siemon et al., 2009). By the variation of resistivity values chemical groundwater status and/or geological features and, thus, aquifer structure can be detected and mapped (Burval Working Group, 2009; Jørgensen and Sandersen, 2009; Jørgensen et al., 2012). Especially groundwater salinization and saltwater intrusion into coastal aquifers provoke high conductivity or low resistivity (Siemon et al., 2007, 2009) and can be detected very well. But, particular care must be taken to distinguish between fluid resistivity and lithology (Günther and Müller-Petke, 2012). Frequency-domain and time-domain airborne applications are available and their worth has been proven during the last 10 yr (Siemon et al., 2009; Steuer et al., 2007).

For Föhr a time-domain airborne transient electromagnetic survey was commissioned by the Leibniz Institute for Applied Geophysics (LIAG) and carried out with the SkyTEM system (Sørensen and Auken, 2004) by SkyTEM ApS in 2008 (Fig. 1d). The whole island (137 km^2) is surveyed in two days including 4 flights, 32 E-W lines adding up to 306 line-km. The nominal flight line spacing of 250 m and the point spacing of 20–30 m between single soundings ensure a good coverage of aquifers, aquitards and saltwater intrusions. High and low transmitter moments (20 750 Am^2, respectively 188 000 Am^2, time gate 10 µs–7 ms) enable a good resolution within a penetration depth of about 30–300 m. The nominal transmitter altitude was about 30 m above ground level and the flight speed about 70–80 $\mathrm{km\,h}^{-1}$. The collected data generally show a good data quality. The apparent resistivity data points are inverted to a resistivity depth distribution. With the assumption of layered strata, the inversion, using 1-D models and lateral or spatial constraints (LCI, respectively SCI), generates an appropriate resistivity model of the subsurface (Auken and Christiansen, 2004; Viezzoli et al., 2008; Christensen et al., 2009). The inversion was carried out by Aarhus Geophysics with 5-layer and smoothed 18-layer resistivity models (Auken et al., 2009).

3.2 Seismic methods

Seismic methods are a good complement to electromagnetic data. They utilize differences in mechanical properties of geologic units. They cannot be used to detect directly saltwater, but they can delineate the boundaries of units which may influence the position and movement of the saltwater interface (Stewart, 1999). With high-resolution seismic surveys using compressional and shear waves (P- and S-waves) detailed structural images of the shallow underground down to 500 m are feasible (Pugin et al., 2009).

For the conversion of seismic time sections into seismic depth sections realistic seismic velocities are crucial. Vertical seismic profiling (VSP) is the appropriate method for in-situ measurements and can be applied in existing groundwater observation wells. VSP velocities are much more accurate than velocities deduced from seismic reflection processing.

On Föhr 2-D high-resolution seismic surveys were carried out by LIAG during 2009 and 2011 (Fig. 1d). All in all, 7 profiles with P-waves (8.0 km), 3 profiles with S-waves (2.4 km) and VSPs with both P- and S-waves in 5 boreholes (maximal depth 39–102 m) were acquired. As seismic sources LIAG's hydraulically driven vibrator systems MHV2.7 and HVP-30 (Buness and Wiederhold, 1999) were used for P-wave and MHV4S (Polom et al., 2010) for S-wave surveys. For VSP measurements the small electro-dynamical vibrator system EVLIS (Polom et al., 2011; Krawczyk et al., 2011) was used as seismic source. Adequately chosen acquisition parameter (Table 1) as well as thorough processing provides good structural images of the subsurface. Processing steps for reflection seismic were, e.g. spectral whitening, dip move-out and normal move-out correction as well as common midpoint stacking (Yilmaz, 2001). Velocity analysis was done in an iterative way resulting in improved velocity depth sections. Time-to-depth conversion was done by a single interval velocity function from VSP (Beo26, Fig. 4) above −100 m m.s.l. and stacking velocity below −100 m m.s.l.

3.3 Borehole logs

To verify seismic and electromagnetic results a direct link to the subsurface is required. Groundwater observation wells and water supply wells are a good basis for the combined interpretation and geological models. The lithology description combined with borehole logging results is the main source for the geological knowledge.

On Föhr a dense borehole coverage exists (Fig. 1d) and provides a good geological background. In 1960 the waterworks started to install pumping and observation well systems via flush drillings. The boreholes reach a maximum depth down to −120 m m.s.l. For most boreholes standard borehole logs are available, e.g. gamma ray and resistivity logs (short and long normal 64″, focussed electrical log FEL).

3.4 Combined analysis

Combined analysis and interpretation provide more reliability to geophysical and geological data for geological modelling. Information transfer among the different geophysical methods or inclusion of geological information leads to matching results for processing (seismic data), inversions or modelling (SkyTEM data).

For the SkyTEM data inversion of Föhr we included depth information of seismic horizons into the inversion process (Burschil et al., 2012). We actualized the inversion model to 6-layers and constrained several features from the seismic results. The improved resistivity distribution was used for parameter correlation and structural analysis of the geology (Sect. 4).

3.5 3-D model

The 3-D model is built up with the GOCAD® software (Paradigm Ltd.). The initial geological model of Föhr is based on the integrated analysis of data from hydrogeological investigations for groundwater exploration and groundwater protection purposes in the past 50 yr (Fig. 3). In a next step the SkyTEM and seismic data are added to the model

(Fig. 3). The early investigations were restricted to the areas around the two waterworks in the eastern and western part of the Geest. In the middle part of the Geest and in the marsh there was a big lack of data concerning geological information as well as data on the freshwater interface. In this context especially the results of the SkyTEM survey delivered a lot of new data. The relevant geological units were elaborated and surfaces were constructed. The morphology of the geological layers has been adapted according to the geophysical data. In total 12 layers are constructed displaying four Pleistocene and two Tertiary aquifers which are covered by five Quaternary and one Tertiary aquitards (Fig. 3).

4 Results

4.1 Petrophysical properties

The high density of geophysical data (SkyTEM, seismic reflection in P- and S-wave configuration, vertical seismic profiles) in connection with the high density of boreholes and logs in the Geest area of Föhr provide a good database for petrophysical considerations that are still a need in hydrogeophysics (e.g. Rubin and Hubbard, 2005; Lesmes and Friedman, 2005; Pride, 2005). These considerations should contribute to improved rock identification and enable the derivation of empirical relationships – at least valid for this specific site – for assessment of hydraulic properties (especially hydraulic conductivity), both based on seismic and resistivity results. The rocks or soils of interest on the Island of Föhr are clay, silt, till (all aquicludes), sand and gravel (both aquifers).

4.1.1 Rock identification

Using electrical resistivity for the discrimination of clayey and clay free sediments seems to be easy since resistivity of clay free sediments follows Archie's law that electrical current flow is predominantly through the pore water (Archie, 1942), while for clayey sediments the surface conductivity of clay minerals plays an important role in the current flow. So formulations to calculate resistivity of clayey sediments have to account for surface conductivity (e.g. Frohlich and Parke, 1989) or cation exchange capacity (e.g. Sen et al., 1988). For freshwater saturated sediments it can be expected that resistivity of clay free sands is higher than resistivity of clayey sediments.

To improve the interpretation of the SkyTEM survey in terms of the geological setting for the Island of Föhr borehole lithology is compared to resistivity values from SkyTEM data (Fig. 4). This is done for 18 boreholes located in the Geest area and deeper than 75 m. If the drilling is not in the immediate vicinity of a SkyTEM flightline, projected datapoints were used. Borehole resistivity values (long normal 64″ and FEL) are used for interpretation. In general, the resistivity measured with the long normal borehole equipment is higher than the corresponding resistivity from the SkyTEM survey and the FEL logging. Anisotropy due to fine layering of the underground can be a possible explanation. If low resistivity layers are embedded in the fine layered ground electrical anisotropy leads to reduced resistivity value for current flow parallel to the layering, while for current flow perpendicular to the layering an increased resistivity is measured. Time domain electromagnetics with horizontal coils like with the SkyTEM-system creates a field of eddy currents for which the predominant flow direction is horizontal, a more or less horizontal current flow is also generated by the FEL logging. This would lead to lower measured resistivity values, while measurements using long normal resistivity borehole equipment with vertical current flow direction would lead to higher resistivity values.

All results (see Fig. 5) have in common that the measured resistivity for sand is higher than the resistivity for clayey material. The resistivity for clay and till is similar. Overlapping resistivity values for sandy and clayey material are in the range of 50–100 Ωm. This can lead to interpretation problems.

Seismic velocities also enable discrimination of sand and till. Direct access to seismic velocities in relation to lithology is given by vertical seismic profiles at five observation wells (Fig. 1d). In Fig. 6 measured seismic velocities for P- and S-waves are shown for sand and till. The velocities of till are in general higher than the velocities of sand, even if an overlapping velocity range exist. P-wave velocities below 1500 $\mathrm{m\,s^{-1}}$ (= P-wave velocity of water) can be explained by the influence of the uppermost dry layers.

A possible explanation for the increased seismic velocity is the reduced porosity of till. If sand and clay are mixed to form till, the tiny clay particles concentrate in the pore space of the sand, reduce the porosity and, by blocking the pore channels, reduce the permeability. This porosity reduction effect was shown by Marion et al. (1992) at laboratory experiments with artificial sand-clay mixtures. The highest seismic velocity was found at about 25 % clay content depending on the confining pressure.

4.1.2 Empirical relationship between resistivity and hydraulic conductivity for the Island of Föhr

For clay free sediments, electrical resistivity is strongly related to porosity. If the pore water resistivity is assumed to be constant, lateral changes of measured resistivity values can be interpreted in terms of changing porosity. To go one step further, for an interpretation of resistivity changes as changes of hydraulic conductivity the complicated relation between porosity and hydraulic conductivity must be taken into account (Lesmes and Friedman, 2005). The key parameter for the determination of hydraulic conductivities is the effective porosity (total porosity reduced by the stagnant water content), while the electrical resistivity is strongly influenced by the entire water content which is – in the saturated case – equivalent to the total porosity. The relation of total to effective porosity depends on grain shape and grain size distribution, it is hardly to predict. As a consequence, positive as well as negative relations between hydraulic conductivities and measured resistivity or formation factors are reported in the literature (e.g. Urish, 1981; Biella et al., 1983; Purvance and Andricevic, 2000). Similar effects were found for the correlation between P-wave velocities, which are also strongly affected by the total porosity, and hydraulic conductivity (Fechner, 1998).

Hydraulic conductivities from pumping test are scarce for the Island of Föhr. To achieve a data base of hydraulic conductivities for comparison with resistivity, we made use of the petrographic description from drilling results (hydraulic circulation drillings). From this description 18 petrographic units were identified (ranging from clay to coarse sand). Mean hydraulic conductivities as known for Northern German soils (DVGW, 1982; Hölting and Coldewey, 2005) were attached to each unit, e.g. $k_f = 1 \times 10^{-4}\,\mathrm{m\,s^{-1}}$ for fine sand or $k_f = 1 \times 10^{-3}\,\mathrm{m\,s^{-1}}$ for coarse sand. These hydraulic conductivities were compared with resistivity values obtained from borehole logs (long normal 64″ and FEL) and from the SkyTEM survey. The so obtained resistivity values were mean averaged for each petrographic unit (Table 2 and Fig. 7). Only resistivity data averaged over at least 50 samples (vertical spacing of samples is 1 m) were used for this comparison. For the clayey material not all variations are included as is seen in Fig. 4 (left panel) where variations in the till are shown in the gamma ray and resistivity logs. For the sandy material a positive correlation between electrical resistivity and hydraulic conductivity is found (Fig. 7). Following Archie's law, the resistivity of clay free material is inversely related to the porosity. So a negative correlation of porosity and hydraulic conductivity can be assumed for the project area. Similar results for Föhr were found by Grabowski (2012) and for the region of Quakenbrück (Niedersachsen) by Klimke (2012).

4.2 Structural interpretation and 3-D model

The seismic sections allow insight into the geological structures down to a depth of at least 400 m (Fig. 9a). We recognize three different geological units (Fig. 10): the more or less horizontal and undisturbed reflections below 150 m represent Tertiary layers. Above 150 m the picture totally changes and the reflection pattern is very complex. Dipping reflections predominate indicating glacial thrust-faulting. This glaciotectonic complex is separated to the undisturbed section by a detachment or decollement horizon. Further upwards, this glaciotectonic complex is partly eroded by glacial incision. This valley is filled with glacial deposits. The seismic velocities allow the delineation of sand and till (Sect. 4.1.1) and by its higher velocity a till layer at the bottom of the valley is detected (Fig. 9b). The combination with the resistivity (Fig. 9c) emphasises the tripartition (valley, glaciotectonic complex and undisturbed Tertiary). Varying resistivity in the thrust-fault complex may indicate thrust sand (Pliocene) and clay (Miocene). This parallel occurrence of sand and clay can also be traced in the resistivity depth slices (Fig. 8). In the northern part of the slices (Fig. 8) and section (Fig. 9c) and below the detachment the very low resistivity point to saltwater occurrence.

The base of the 3-D model (Figs. 3, 11) consists of Miocene clay that is covered by the two Tertiary aquifers, which in some areas are separated by a clayey aquitard. The interpretation of the seismic sections (Figs. 9, 10) has shown that the bedding of the Tertiary strata is strongly affected by glacial tectonics down to a depth of about −150 m m.s.l. As a result of the ice pressure a pattern of elongated sand bodies of Pliocene Kaolin sand alternating with Miocene clay exists, which can be seen in east to west direction in the SkyTEM data too (see Fig. 8). To integrate these sand bodies as aquifers in the model, their spatial extension was derived from the resistivity data.

The depth of the Quaternary strata varies strongly (Figs. 2, 11). In some areas of the Western Geest only Pleistocene cover of 10 to 20 m thickness exists. Quaternary sediments in buried valleys reach depths of more than −130 m m.s.l. The course of the two buried valleys in the eastern part of the island corresponds with the south-north direction of the glacial thrust structures in the Tertiary strata (Figs. 8b, 11).

The fill of the valleys and the deeper part of the Quaternary sediments outside of the valleys mainly consist of fine grained material like clay, silt and till as known from boreholes.

The near surface Quaternary strata is built up by Saalian meltwater sands, which in wide areas, form a non-covered aquifer in the Geest of the island, which is hydraulically connected to the 2nd Quaternary aquifer. The 1st and the 2nd aquifer are the production horizon of nearly all wells of the waterworks. In the marsh the 1st aquifer is covered by some meters of Holocene clay.

5 Discussion

Borehole information and results from geophysical measurements enable the compilation of the geological/hydrogeological 3-D model. The quality of the assembled data and the experience of the modelling geologist are the major aspects that justify the reality and reliability of the generated model. In the following the data quality is discussed.

Our geophysical data bear a generally good data quality. The SkyTEM data show a low noise level. During processing of SkyTEM data, couplings caused by man-made structures and soundings with poor quality were eliminated leading to a proper resistivity model. This is the reason for less resistivity data density in the urban area of the Eastern Geest. Electromagnetic methods, especially airborne EM, have methodical limits as dispersive method. The resultant resistivity distribution reflects an integrated volume in the subsurface with decreasing resolution in depth (Høyer et al., 2011). The inversion algorithm claims more or less horizontal layered environments when using spatial constraints (Auken and Christiansen, 2004). Steep dipping or vertical resistivity contrasts will not be resolved and are shown as smooth transitions. Depending on this limitation and the width of the footprint horizontal resolution is limited. The quality of inversion is evaluated further by Burschil et al. (2012).

Our results from seismic reflections have a good signal/noise ratio and show P-wave reflections down to -700 m m.s.l. The applied processing scheme was relatively robust while small changes have no large effects to the seismic section. The reflections correlate with layer boundaries in affiliated boreholes and characterized structures in 2-D.

The petrophysical interpretation is based on borehole data (electrical logs and VSPs). Regarding the seismic velocity a clear discrimination of sand and till is possible with a mean P-wave velocity value for sand about $1675\,\mathrm{m\,s^{-1}}$ and for till about $1950\,\mathrm{m\,s^{-1}}$. The interpretation of interval velocities determined from stacking velocities is generally problematic. But due to the good correlation with borehole data (Figs. 4, right panel, and 10) we consider the interpretation of the till layer appropriate (Fig. 9b). Concerning the resistivity, a clear discrimination between sand and till (Fig. 5) is possible using borehole data (long normal 64″, FEL). Using SkyTEM data, some overlapping of resistivities for sand and clay occur. A possible reason is that the SkyTEM results had to be projected to the borehole locations (interpolation between flightlines) resulting in reduced resistivity resolution.

The 3-D model constructor has to consider the reliability of the data. Usually all data from boreholes, seismic cross sections and boundaries in the resistivity models does not fit exactly together. The task is to produce a 3-D model from 1-D borehole data, 2-D seismic cross sections and 3-D resistivity models consisting of a bundle of 1-D resistivity models. At the end, the model should fit all data and even agree with a plausible geological genesis. This is – in our opinion – the case for the presented model of the Island of Föhr. The interpretation of thrust-faulting and its imaging in the combination of seismic and resistivity data is unique. Thrust-faulting is known for Northern Germany and imaged quite well in marine seismic sections offshore the North Frisian Islands (e.g. Koopmann et al., 2010; Andersen, 2004) but onshore imaging is scarce. Indications to glaciotectonic complexes are presented by Jørgensen et al. (2012) or, further east, in Poland, by Morawski (2004).

We are aware of the fact that our geologic structures are very complex and cannot be included in detail in a groundwater model (Voss, 2011a,b). Initial results of hydraulic groundwater modeling including the effects of the forecasted climate changes like changes in precipitation and sea level rise show the development of the water balance until the year 2100 (LLUR, 2012).

6 Conclusions

We have demonstrated that geophysical investigation can provide petrophysical parameters and can improve the geological/hydrogeological model and thus the understanding of the subsurface and the groundwater system. Especially seismic reflection data in combination with airborne EM (SkyTEM) and in combination with borehole information enhance the hydrogeological characterization regarding rock identification and structure and thus the 3-D model of the subsurface of the Island of Föhr. The SkyTEM data improve the knowledge concerning geological information as well as data on the freshwater interface for areas outside and in between the eastern and western part of the Geest to where previous work was restricted. The extent of the freshwater occurence is determined as well as the freshwater-saltwater boundary and the extent of glaciotectonic structures. The structural interpretation is improved by rock identification. An empirical relationship between electric and hydraulical properties is determined for this specific site, the Island of Föhr, the use of this has to be evaluated in future work.

The main benefit of our work is that by the fruitful combination of EM, seismic and borehole data it is possible to reveal this complex geology and to improve our understanding and spatial resolution of glacially affected regions that will have a strong impact on the groundwater flow system.

Acknowledgements. We thank Flemming Jørgensen for fruitful discussion and the initial idea of glacial overprinting. Further we thank Hark Ketelsen and the “Wasserbeschaffungsverband Föhr” for support during our geophysical surveys as well as Bernd König and Anja Wolf from LLUR. We also acknowledge LIAG’s seismic field crew for their excellent work during the surveys.

This article is an outcome of the EU Interreg IVB project CLIWAT (ID 35-2-1-08). It has been co-funded by the North Sea Region Programme 2007–2013 under the ERDF of the European Union.

References

Aber, J. S. and Ber, A.: Glaciotectonism. Developments in Quaternary Sciences, 1st Edn., Elsevier, Amsterdam, 2007.

Andersen, L. T.: The Fanø Bugt Glaciotectonic Thrust Fault Complex, Southeastern Danish North Sea – A study of large-scale glaciotectonics using high-resolution seismic data and numerical modeling, Ph.D. thesis, Danmarks og Grønlands Geologiske Undersøgele Rapport 2004/30, Copenhagen, 2004.

Archie, G. E.: The electrical resistivity log as an aid in determining some reservoir characteristics, T. Am. I. Min. Met. Eng., 146, 54–62, 1942.

Auken, E. and Christiansen, A. V.: Layered and laterally constrained 2-D inversion of resistivity data, Geophysics, 69, 752–761, doi:10.1190/1.1759461, 2004.

Auken, E., Christiansen, A. V., Westergaard, J. H., Kirkegaard, C., Foged, N., and Viezzoli, A.: An integrated processing scheme for high-resolution airborne electromagnetic surveys, the SkyTEM system, Explor. Geophys., 40, 184–192, 2009.

Biella, G., Lozej, A., and Tabacco, I.: Experimental study of some hydrogeophysical properties of unconsolidated porous media, Ground Water, 21, 741–751, 1983.

Buness, H. and Wiederhold, H.: Experiences with a vibrator system for shallow high-resolution seismic, Ext. Abst., EAGE 61st Conference and Technical Exhibition, Helsinki, 1999.

Burschil, T., Wiederhold, H., and Auken, E.: Seismic results as a-priori knowledge for airborne TEM data inversion – a case study, J. Appl. Geophys., 80, 121–128, doi:10.1016/j.jappgeo.2012.02.003, 2012.

BURVAL Working Group: Buried quaternary valleys – a geophysical approach, Z. dtsch. Ges. Geowiss., 160, 237–247, 2009.

Christensen, N. B., Reid, J. E., and Halkjær, M.: Fast, laterally smooth inversion of airborne time-domain electromagnetic data, Near Surf. Geophys., 7, 599–612, 2009.

Christiansen, A. V., Auken, E., and Sørensen, K.: The transient electromagnetic method, in: Groundwater Geophysics – A tool for Hydrogeology, 2nd Edn., edited by: Kirsch, R., Springer, Heidelberg, 398–413, 2009.

DVGW: Ermittlung des nutzbaren Grundwasserdargebots, Schriftenreihe des Deutschen Verbandes für Wasserwirtschaft und Kulturbau e.V., 58, 1982.

European Commission: Common implementation strategy for the water framework directive (2000/60/EC), Guidance document No. 24, River basin management in a changing climate, Technical Report 40, Luxembourg, 2009.

Fechner, T.: Seismische Tomographie zur Beschreibung heterogener Grundwasserleiter, Tübinger Geowissenschaftliche Arbeiten, C40, Tübingen, 1998.

Fountain, D.: Airborne electromagnetic systems 50 yr of development, Explor. Geophys., 29, 1–11, 1998.

Frohlich, R. K. and Parke, C. D.: The electrical resistivity of the vadose zone – field study, Ground Water, 27, 525–530, 1989.

Grabowski, I.: Ableitung hydraulischer und thermischer Untergrundparameter aus elektromagnetischen Messungen am Beispiel der Insel Föhr, Diplomarbeit, Institut für Geowissenschaften der Christian-Albrechts-Universität Kiel, 2012.

Green, T. R., Taniguchi, M., Kooi, H., Gurdak, J. J., Allen, D. M., Hiscock, K. M., Treidel, H., and Aureli, A.: Beneath the surface of global change: impacts of climate change on groundwater, J. Hydrol., 405, 532–560, 2011.

Gripp, K.: Erdgeschichte von Schleswig-Holstein, Wachholz Verlag, Neumünster, 1964.

Grube, A.: Grundwasserversalzung in der Norddeutschen Tiefebene, Band 9, DVGW-Technologiezentrum Wasser, Karlsruhe, 2000.

Günther, T. and Müller-Petke, M.: Hydraulic properties at the North Sea island Borkum derived from joint inversion of magnetic resonance and electrical resistivity soundings, Hydrol. Earth Syst. Sci. Discuss., 9, 2797–2829, doi:10.5194/hessd-9-2797-2012, 2012.

Gürs, K.: Das Tertiär Norddeutschlands in der Stratigraphischen Tabelle von Deutschland 2002, Newsl. Stratigr., Berlin Stuttgart, 2005.

Hölting, B. and Coldewey, G. C.: Hydrogeologie – Einführung in die Allgemeine und Angewandte Hydrogeologie, 6th Edn., Elsevier, München, 2005.

Holman, I. P., Allen, D. M., Cuthbert, M. O., and Goderniaux, P.: Towards best practice for assessing the impacts of climate change on groundwater, Hydrogeol. J., 20, 1–4, 2012.

Høyer, A. S., Lykke-Andersen, H., Jørgensen, F., and Auken, A.: Combined interpretation of SkyTEM and high-resolution seismic data, J. Phys. Chem. Earth, 36, 1386–1397, doi:10.1016/j.pce.2011.01.001, 2011.

Jørgensen, F. and Sandersen, P. B. E.: Buried valley mapping in Denmark: evaluating mapping method constraints and the importance of data density, Z. dtsch. Ges. Geowiss., 160, 211–223, 2009.

Jørgensen, F., Scheer, W., Thomsen, S., Sonnenborg, T. O., Hinsby, K., Wiederhold, H., Schamper, C., Burschil, T., Roth, B., Kirsch, R., and Auken, E.: Transboundary geophysical mapping of geological elements and salinity distribution critical for the assessment of future sea water intrusion in response to sea level rise, Hydrol. Earth Syst. Sci. Discuss., 9, 2629–2674, doi:10.5194/hessd-9-2629-2012, 2012.

Klimke, J.: Erstellung eines geologisch – geophysikalischen Untergrundmodells für den Bereich des pleistozänen Quakenbrücker Beckens in Niedersachsen, Masterarbeit, Institut für Geologie der Leibniz Universität Hannover, 2012.

Koopmann, H., Gaedicke, C., and Lutz, R.: The glaciotectonic thrust-fault complex north of Heligoland, Tagungsband 70. Jahrestagung Deutsche Geophysikalische Gesellschaft, Bochum, 92, 2010.

Krawczyk, C. M., Polom, U., Trabs, S., and Dahm, T.: Sinkholes in the city of Hamburg – new urban shear-wave reflection seismic system enables high-resolution imaging of subrosion structures, J. Appl. Geophys., 78, 133–143, doi:10.1016/j.jappgeo.2011.02.003, 2011.

Lesmes, D. P. and Friedman, S. P.: Relationships between the electrical and hydrogeological properties of rocks and soils, in: Hydrogeophysics, edited by: Rubin, Y. and Hubbard, S. S., Springer, Dordrecht, 87–128, 2005.

Littke, R., Bayer, U., Gajewski, D., and Nelskamp, S.: Dynamics of Complex Intracontinental Basins – the Central European Basin System, Springer, Berlin, 2008.

LLUR: Der Untergrund von Föhr: Geologie, Grundwasser und Erdwärme, Ergebnisse des INTERREG-Projekts CLIWAT, Schriftenreihe LLUR SH – Geologie und Boden 18, Landesamt für Landwirtschaft, Umwelt und Ländliche Räume Schleswig-Holstein, Flintbek, 102 pp., 2012.

Marion, D., Nur, A., Yin, H., and Han, D.: Compressional velocity and porosity in sand-clay mixtures, Geophysics, 57, 554–563, 1992.

Morawski, W.: Glaciotectonic structures of the Southern Warmia region (Poland), in: The Application of Geophysical Methods in the Study of Cenozoic Deposits and Glaciotectonic Deformations as Exemplified by the Southern Warmian Region (Poland), edited by: Morawski, W., Prace Panstwowego Instytutu Geologicznego 180, Warszawa, 109–141, 2004.

Paine, J. G. and Minty, B. R. S.: Airborne Hydrogeophysics, in: Hydrogeophysics, edited by: Rubin, Y. and Hubbard, S. S., Springer, Dordrecht, 333–357, 2005.

Polom, U., Hansen, L., Sauvin, G., L'Heureux, J. S., Lecomte, I., Krawczyk, C., Vanneste, M., and Longva, O.: High-resolution SH-wave seismic reflection for characterization of onshore ground conditions in the Trondheim Harbor, Central Norway, in: Advances in Near-Surface Seismology and Ground-Penetrating Radar, edited by: Miller, R. D., Bradford, J. D., and Holliger, K., SEG, Tulsa, 297–312, 2010.

Polom, U., Druivenga, G., Großmann, E., Grüneberg, S., and Rode, W.: Transportabler Scherwellenvibrator, DPMA Patentschrift DE10327757B4, München, 26 May 2011.

Pride, S. R.: Relationships between seismic and hydrological properties, in: Hydrogeophysics, edited by: Rubin, Y. and Hubbard, S. S., Springer, Dordrecht, 253–290, 2005.

Pugin, A. J. M., Pullan, S. E., Hunter, J. A., and Oldenborger, G. A.: Hydrogeological prospecting using P- and S-wave landstreamer seismic reflection methods, Near Surf. Geophys., 7, 315–327, 2009.

Purvence, D. T. and Andricevic, R.: On the electrical-hydraulic conductivity correlation in aquifers, Water Resour. Res., 36, 2905–2913, 2000.

Rubin, Y., Hubbard, S. S. (Eds.): Hydrogeophysics, Springer, Dordrecht, 2005.

Sen, P. N., Goode, P. A., and Sibbit, A.: Electrical conduction in clay bearing sandstones at low and high salinities, J. Appl. Phys., 63, 4832–4840, 1988.

Siemon, B., Steuer, A., Meyer, U., and Rehli, H.-J.: HELP-ACEH – a post-tsunami helicopter-borne groundwater project along the coasts of Aceh, Northern Sumatra, Near Surf. Geophys., 5, 231–240, 2007.

Siemon, B., Christiansen, A. V., and Auken, E.: A review of helicopter-borne electromagnetic methods for groundwater exploration, Near Surf. Geophys., 7, 629–646, 2009.

Sørensen, K. I. and Auken, E.: SkyTEM – a new high-resolution helicopter transient electromagnetic system, Explor. Geophys., 35, 191–199, 2004.

Steuer, A., Siemon, B., and Auken, E.: A comparison of helicopter-borne electromagnetics in frequency- and time-domain at the Cuxhaven valley in Northern Germany, J. Appl. Geophys., 67, 194–205, 2007.

Stewart, M. T.: Geophysical investigations, in: Seawater Intrusion in Coastal Aquifers, edited by: Bear, J., Cheng, A., Sorek, S., Ouazar, D., and Herrera, I., Kluwer Academic Publishers, 9–50, 1999.

StUA Schleswig: Hydrogeologischer Bericht zur Bemessung von Wasserschutzgebieten für die Wasserwerke Föhr-Ost und -West des Wasserbeschaffungsverbandes Föhr, Report, Staatliches Umweltamt Schleswig, Schleswig, 83 pp., 2006.

Sulzbacher, H., Wiederhold, H., Siemon, B., Grinat, M., Igel, J., Burschil, T., Günther, T., and Hinsby, K.: Numerical modelling of climate change impacts on freshwater lenses on the North Sea Island of Borkum, Hydrol. Earth Syst. Sci. Discuss., 9, 3473–3525, doi:10.5194/hessd-9-3473-2012, 2012.

Urish, D. W.: Electrical resistivity-hydraulic conductivity relationships in glacial outwash aquifers, Water Resour. Res., 17, 1401–1408, 1981.

Viezzoli, A., Christiansen, A. V., Auken, E., and Sørensen, K.: Quasi-3-D modeling of airborne TEM data by spatially constrained inversion, Geophysics, 73, F105–F113, 2008.

Voss, C.: Editor's message: groundwater modeling fantasies – part 1, adrift in the details, Hydrogeol. J., 19, 1281–1284, 2011a.

Voss, C.,: Editor's message: groundwater modeling fantasies – part 2, down to earth, Hydrogeol. J., 19, 1281–1284, 2011b.

Yilmaz, Ö.: Seismic data analysis: processing, inversion and interpretation of seismic data, Soc. Explor. Geophys., Tulsa, 2001.

Table 1. Acquisition parameter for seismic surveys.

	P-wave	S-wave	VSP
Receiver	planted z-geophones Sensor SM7 (20 Hz)	LIAG landstreamer with SH-geophones (10 Hz)	borehole geophone Geostuff (3-components, 14 Hz)
Receiver spacing	2 m	1 m	1 m
Source	MHV2,7/HVP-30	MHV4S	MHV2,7/ELVIS-6
Source spacing	4 m	4 m	constant
Sweep	30–240 Hz, 10 s	30–160 Hz, 10 s	30–160 Hz, 10 s*
Common-Midpoint spacing	1 m	0.5 m	–

* Sweep frequency and length were adjusted during the surveys.

Table 2. Petrophysical parameter: Mean values of resistivity and seismic velocities for petrographical classification. Mean value (Number of values) is bold.

Petrography	Rho (long normal 64″) [Ωm]	Rho (FEL) [Ωm]	Rho (SkyTEM) [Ωm]	Vp [$\mathrm{m\,s^{-1}}$]	Vs [$\mathrm{m\,s^{-1}}$]
Clay (class. 2)	**45.4** (86)	**24.8** (84)	**23.6** (169)	**1830.4** (52)	**436.5** (52)
Till (class. 5)	**55.6** (409)	**29.8** (289)	**64.0** (454)	**1934.2** (80)	**480.0** (80)
Sand (class. 9–12, 14, 16)	**212.4** (584)	**85.5** (388)	**118.7** (999)	**1523.9** (237)	**334.6** (237)

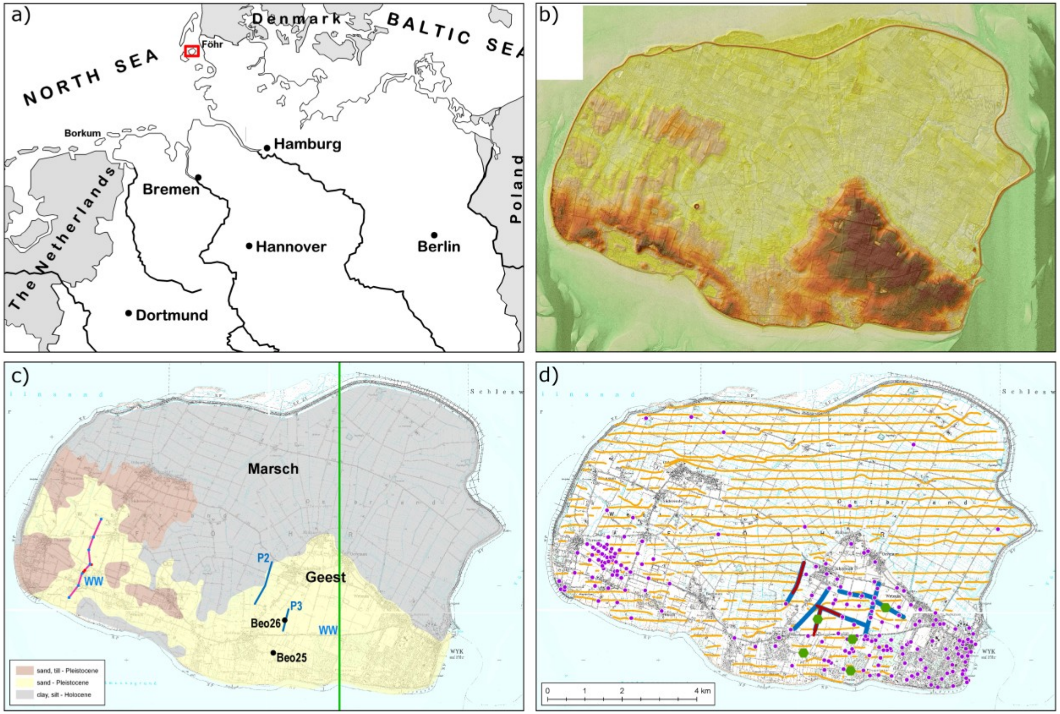

Fig. 1. **(a)** Overview map of Northern Germany. The red box marks the location of Föhr. **(b)** Hypsometric map of Föhr (dark greens for lower elevations up through yellows/browns to higher elevations); **(c)** Geological map of the near surface layers (Geest: brown, yellow; marsh: grey), location of the waterworks (blue WW), geological cross-section (purple line; Fig. 2), boreholes (black dot; Fig. 4), seismic depth-section (blue line; Fig. 9), and model cross section (green line; Fig. 11); **(d)** Geophysical surveys (SkyTEM flightlines: yellow, P-wave seismic reflection lines: blue, S-wave seismic reflection lines: red, boreholes with vertical seismic profiles: green) and boreholes (purple).

HESSD

9, 5085–5119, 2012

Hydrogeological characterisation of a glacially affected barrier island

T. Burschil et al.

Title Page
Abstract | Introduction
Conclusions | References
Tables | Figures
◀| |▶
◀ ▶
Back | Close
Full Screen / Esc
Printer-friendly Version
Interactive Discussion

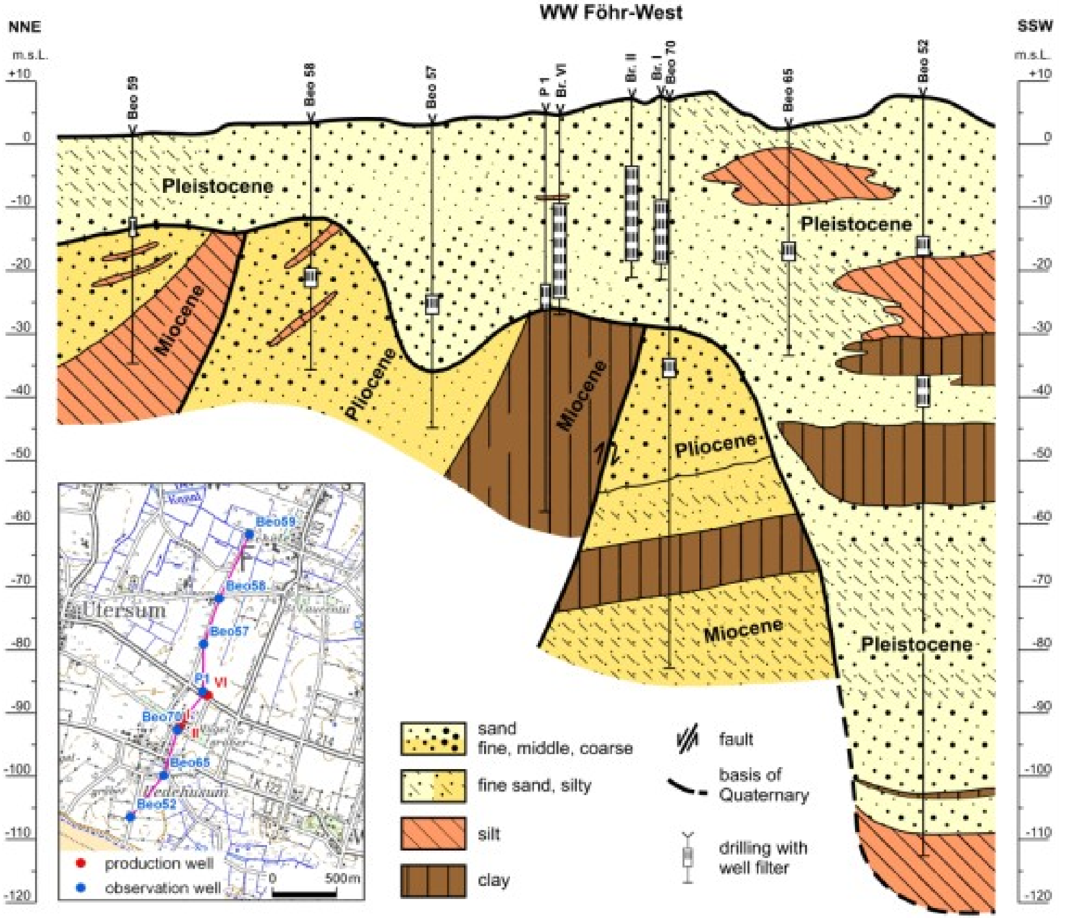

Fig. 2. Geological cross section (based on boreholes and logs) of the Western Geest showing a buried valley and thrust structures in the Miocene strata caused by glaciotectonic processes. The location of the cross section is shown in Fig. 1c.

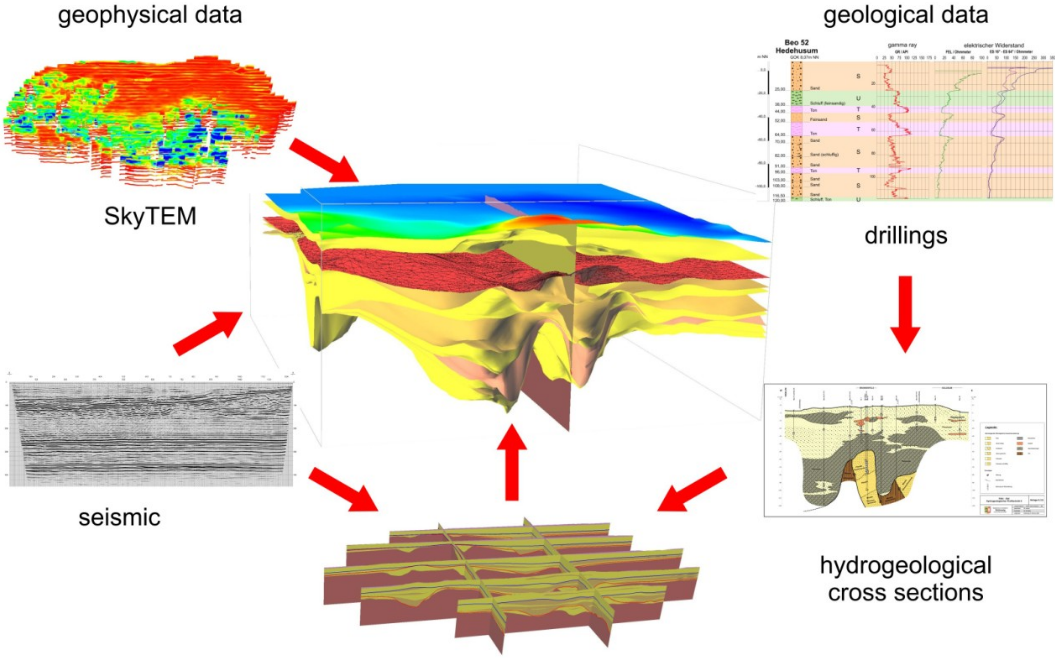

Fig. 3. Layout and data base of the 3-D geological model (cut-out of the central part of the model).

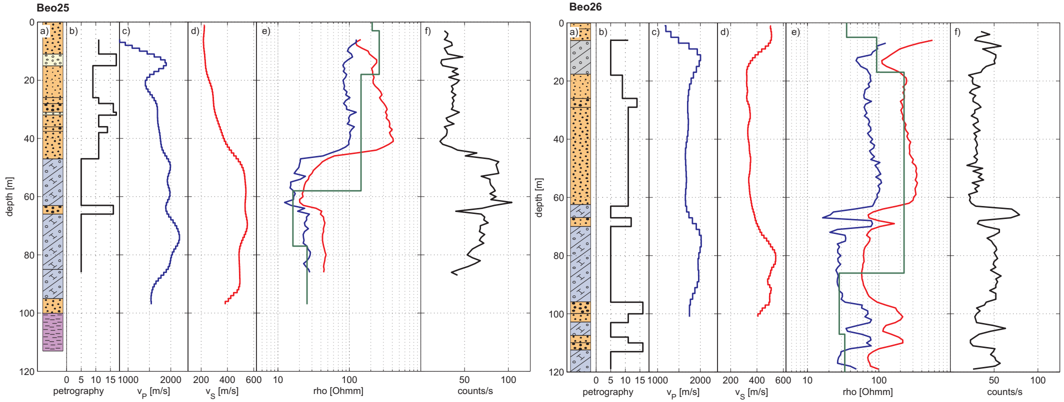

Fig. 4. Example logs for borehole Beo25 (left panel) and Beo26 (right panel) (see Fig. 1c): (a) Lithology (yellow: sand, blue: till), (b) Petrographical classification (1–2: clay, 3–4: silt, 5–6: till, 7–18 fine to coarse sand); (c) P-wave seismic interval velocity from VSP; (d) S-wave seismic interval velocity from VSP; (e) resistivity values for long normal 64″ (red), FEL (blue) and nearby SkyTEM inversion model (green) with offset (Beo25: 177 m; Beo26: 13 m); (f) gamma ray log. Note that the SkyTEM resistivity values do not fit exactly to the resistivity logs due to the horizontal offset of the SkyTEM data points and the large integration volume of this method. For Beo25 the two till layers differ in resistivity as well as gamma log.

Title Page
Abstract
Introduction
Conclusions
References
Tables
Figures
◀
◀
Back
Close
Full Screen / Esc
Printer-friendly Version
Interactive Discussion

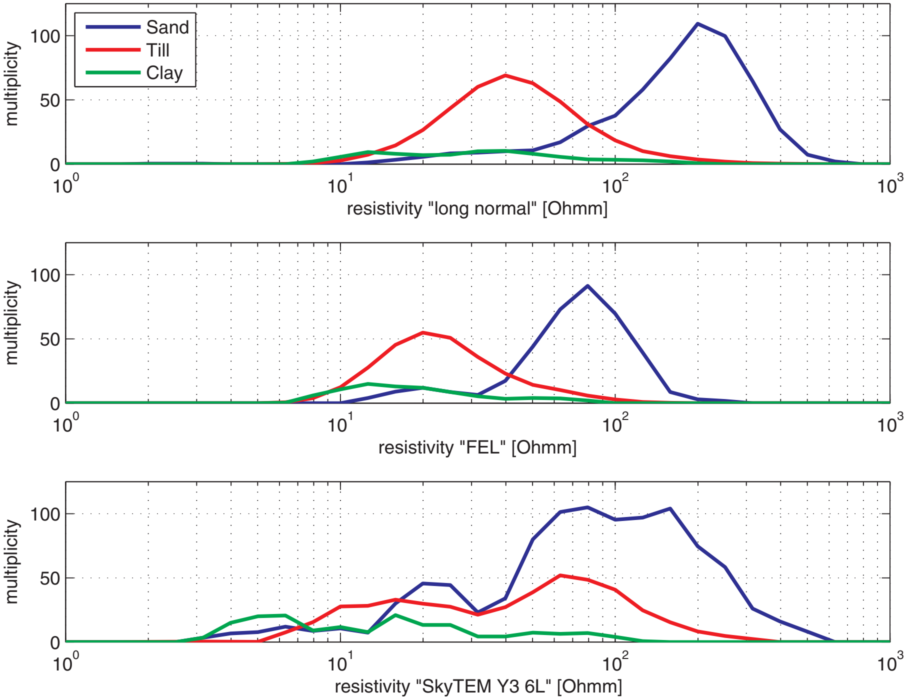

Fig. 5. Histogram of resistivity values from borehole logs and projected SkyTEM resistivity values for petrographical classification of sand, till and clay. Top panel: long normal 64″; middle panel: FEL; bottom panel: 6L model of constrained SkyTEM data. Bins are logarithmically equidistant.

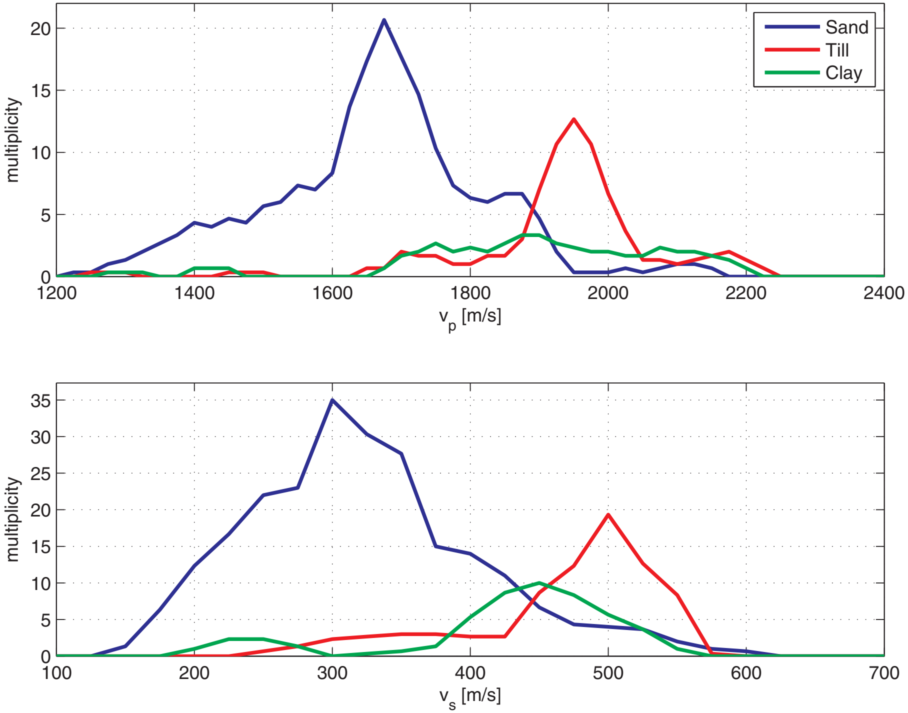

Fig. 6. Histogram of seismic velocities from VSP data for petrographical classification of sand, till and clay. Top panel: P-wave velocities, bottom panel: S-wave velocities.

Title Page
Abstract
Introduction
Conclusions
References
Tables
Figures
◀▌
▶▌
◀
▶
Back
Close
Full Screen / Esc
Printer-friendly Version
Interactive Discussion

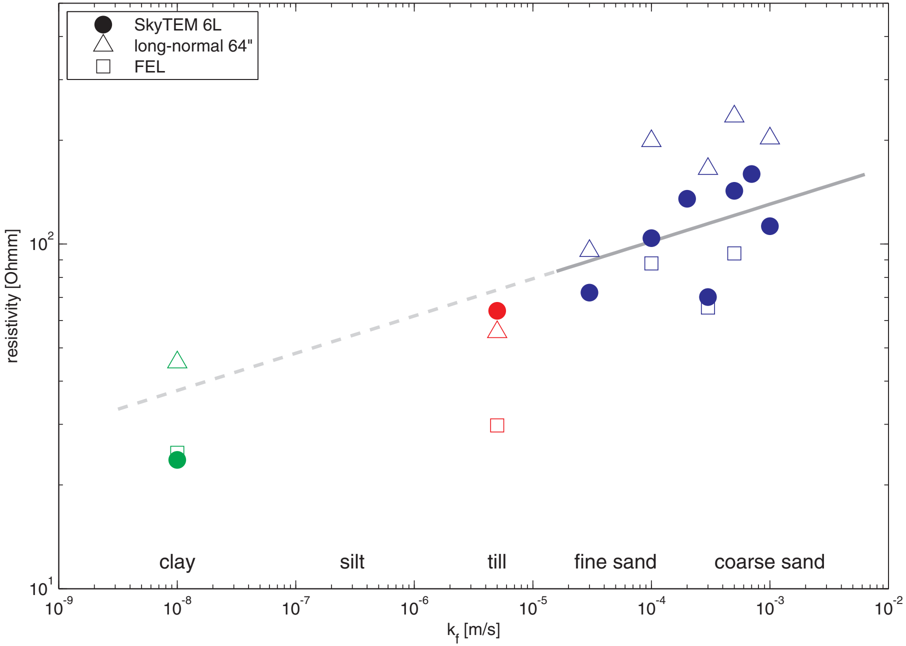

Fig. 7. Correlation between hydraulic conductivity k_f (from petrographical classification after Hölting and Coldewey, 2005; DVGW, 1982) and mean resistivity from constrained SkyTEM data (filled circles). Also mean resistivity values for borehole logs long normal 64″ (triangles) and FEL (squares) are shown. The grey correlation line refers to SkyTEM data within sand (blue filled circles). The colours differ between clay (green), till (red) and sand (blue).

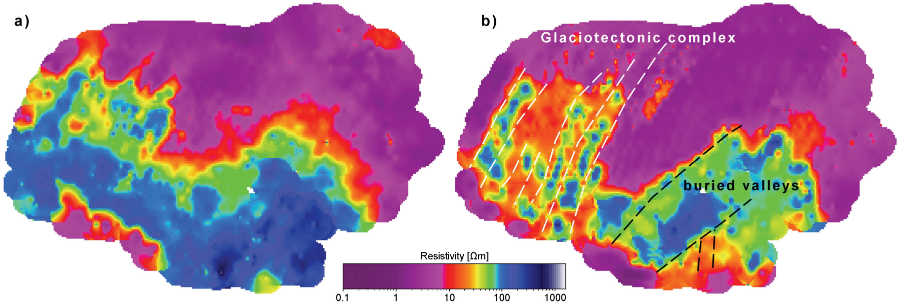

Fig. 8. Resistivity depth slices from SkyTEM data: **(a)** mean resistivity between 0–−10 m m.s.l.; **(b)** mean resistivity between −40–−50 m m.s.l. and interpretation of thrust-fault complex (white) and buried valleys (black).

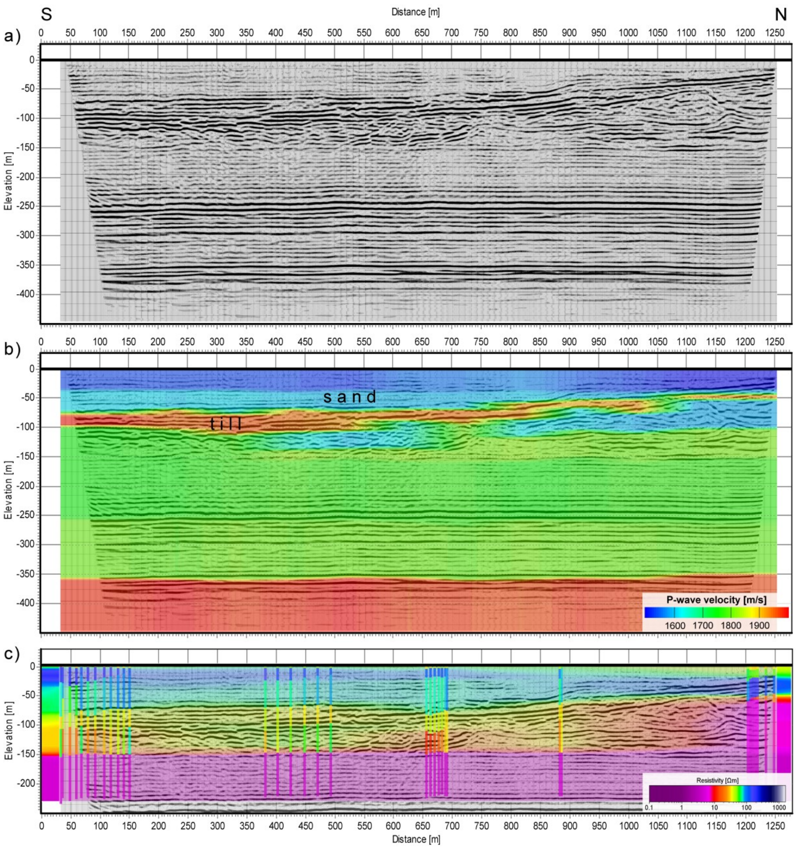

Fig. 9. (a) Seismic depth section (profile P2); **(b)** seismic depth section with interval velocities, **(c)** seismic depth section combined with resistivity data (columns represent 1-D inversion results within 100 m radius to the profile, background colour is from interpolated grid). The location of the profile is shown in Fig. 1c.

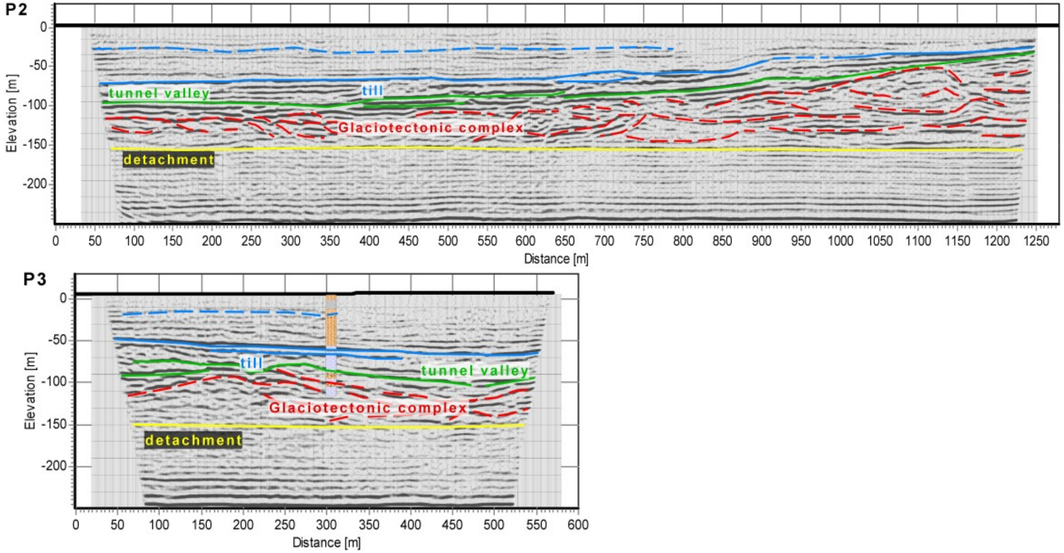

Fig. 10. Interpreted seismic depth sections (profile P2 and P3, see Fig. 1c). Borehole Beo26 (see Fig. 4) is located on profile P3.

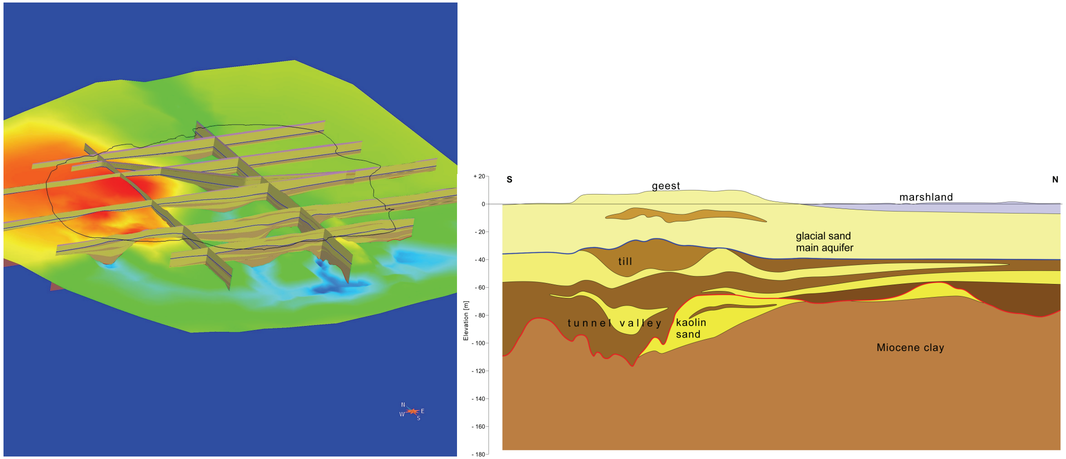

Fig. 11. Left panel: Base of Quaternary (model layer 9, base 5th aquiclude). Right panel: 10 km long cross section through the geological model, yellow: aquifers, brown: aquitards, bluish grey: Holocene clay; depth: −175 m m.s.l.; the blue line marks the basis of the 2nd aquifer; the red line marks the basis of the Quaternary strata; the location of the section is shown in Fig. 1c.